Supporting information for:

Towards high efficiency air-processed near-infrared responsive photovoltaics: bulk heterojunction solar cells based on PbS/CdS core-shell quantum dots and TiO_2 nanorod arrays

Belete Atomsa Gonfa[a], Mee Rahn Kim[a], Nazar Delegan[a], Ana C. Tavares[a], Ricardo Izquierdo[b], Nianqiang Wu[c], My Ali El Khakani[a], and Dongling Ma*[a]

[a]Institut National de la Recherche Scientifique (INRS), Centre-Énergie, Matériaux et Télécommunications, 1650 Boulevard Lionel-Boulet, Varennes, QC, Canada J3X 1S2

[b]Département d'informatique, University of Quebec at Montreal (UQAM), Case postale 8888, succursale Centre-ville, Montréal, Québec H3C 3P8, Canada

[c]Department of Mechanical and Aerospace Engineering, West Virginia University, Morgantown, WV 26506-6106, USA

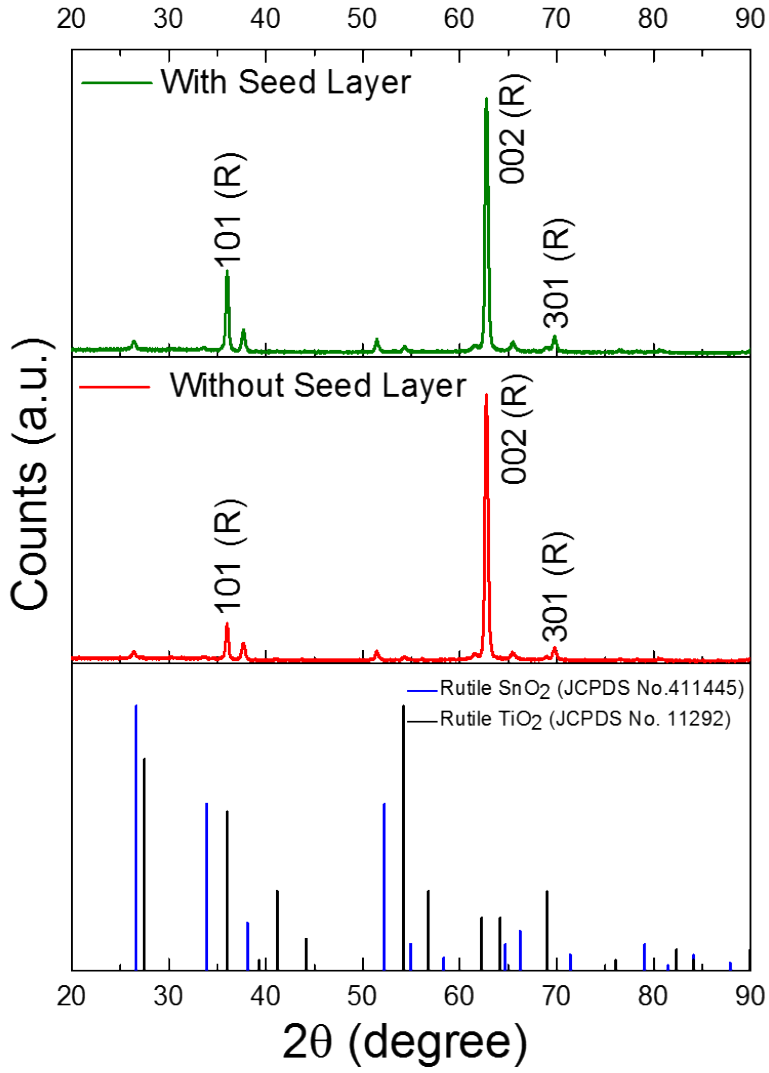

Figure S1. XRD patterns of 2 µm-long TiO_2 nanorod arrays grown on FTO with and without a seed layer, compared with JCPDS files of rutile SnO_2 and rutile TiO_2. R refers to rutile TiO_2.

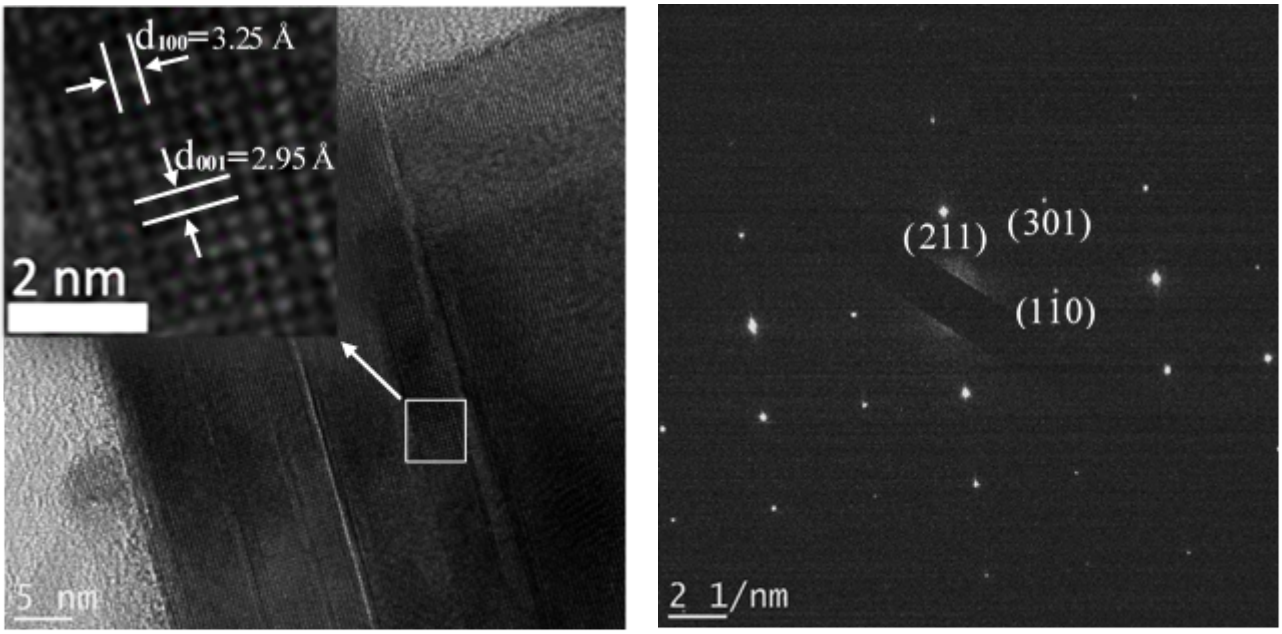

Figure S2. HRTEM images and SAED pattern of a TiO_2 nanorod.

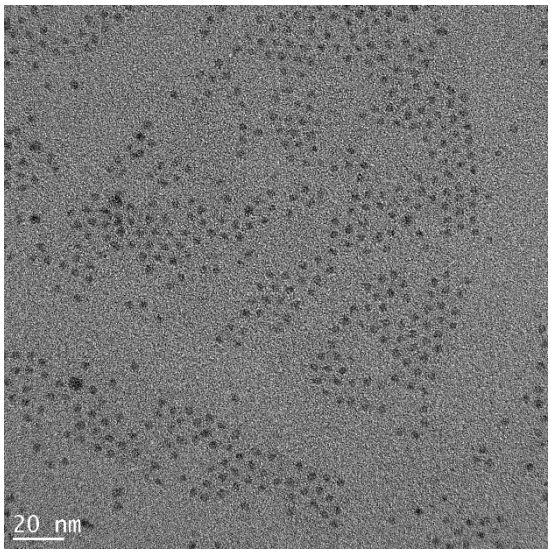

Figure S3. Low magnification TEM image of PbS/CdS core-shell QDs.

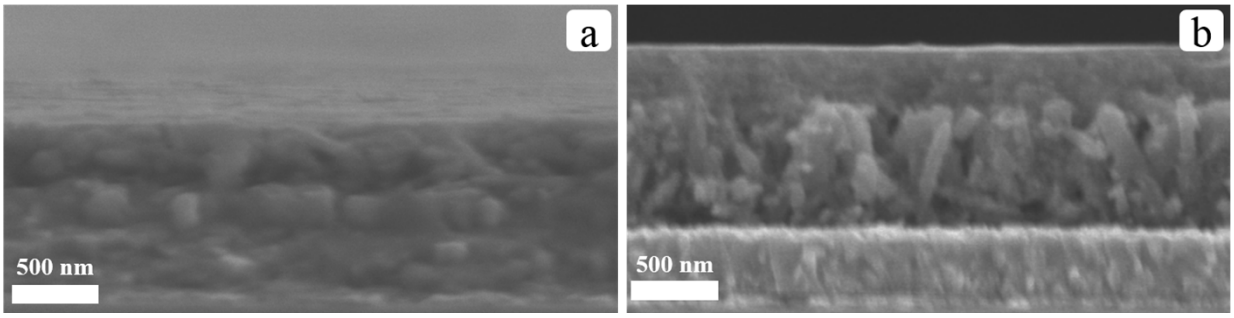

Figure S4. Cross-sectional SEM images of PbS/CdS core-shell QDs spin coated on (a) 250 nm TiO_2 nanorod arrays grown on seed/FTO glass substrate and (b) 650 nm TiO_2 nanorod arrays grown on FTO glass substrate.

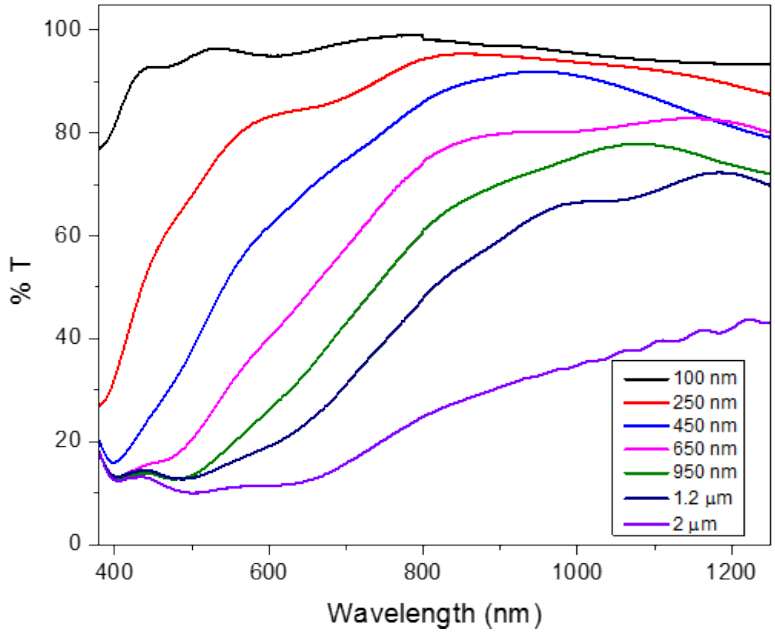

Figure S5. Optical transmittance of TiO_2 nanorod arrays of different length grown on seed/FTO substrate.

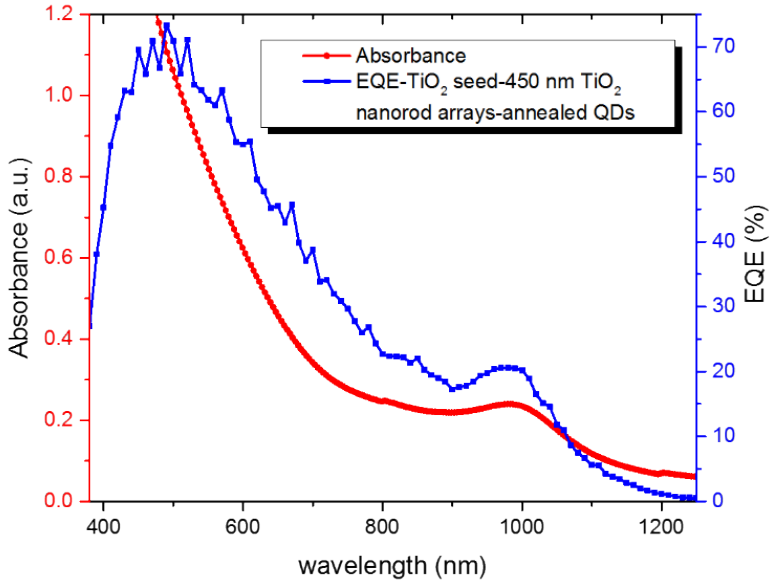

Figure S6. EQE spectrum of the device involving 450 nm TiO_2 nanorod arrays grown on seed/FTO glass substrate and annealed in N_2 atmosphere, compared with the absorption spectrum of annealed PbS/CdS core-shell QDs on quartz.

Table S1. Performance of bulk heterojunction solar cell devices fabricated using TiO_2 nanorod arrays of different length grown on bare FTO substrate.

TiO_2 nanorod array length	**J_{sc} (mA/cm^2)**	**V_{oc} (mV)**	**FF (%)**	**η (%)**
100 nm	12.20 (11.36 ± 0.60)	549 (513 ± 19)	44 (39 ± 2.9)	2.66 (2.46 ± 0.19)
250 nm	13.93 (13.38 ± 0.29)	537 (517 ± 14)	48 (45 ± 2.0)	3.45 (3.19 ± 0.21)
450 nm	13.74 (12.77 ± 0.43)	543 (523 ± 10)	50 (46 ± 2.4)	3.56 (3.25 ± 0.22)
650 nm	13.68 (13.29 ± 0.31)	537 (516 ± 13)	47 (43 ± 2.4)	3.34 (3.11 ± 0.21)
950 nm	13.95 (13.55 ± 0.30)	507 (477 ± 19)	45 (43 ± 2.0)	3.16 (2.85 ± 0.27)
1.2 □m	13.21 (12.73 ± 0.39)	497 (474 ± 14)	43 (39 ± 2.1)	2.69 (2.34 ± 0.25)
2 □m	13.87 (13.04 ± 0.58)	495 (478 ± 11)	37 (33 ± 2.4)	2.41 (2.02 ± 0.19)

Table S2. Performance of bulk heterojunction solar cell devices fabricated using 450 nm-long TiO_2 nanorod arrays grown on the bare FTO and seed/FTO substrates, before and after annealing.

Seed	**Annealing**	**J_{sc} (mA/cm^2)**	**V_{oc} (mV)**	**FF (%)**	**η (%)**
No	No	13.74 (12.77 ± 0.43)	543 (523 ± 10)	50 (46 ± 2.4)	3.56 (3.25 ± 0.22)
No	In N_2	17.69 (17.00 ± 0.37)	493 (481 ± 7)	49 (45 ± 2.4)	4.13 (3.93 ± 0.13)
Yes	No	13.68 (13.29 ± 0.28)	547 (537 ± 6)	52 (48 ± 2.2)	3.76 (3.55 ± 0.17)
Yes	In N_2	17.75 (16.83 ± 0.43)	519 (506 ± 10)	50 (46 ± 2.7)	4.43 (4.28 ± 0.12)